Spray Characteristics on the Electrostatic Rotating Bell Applicator

Kyoung-Su Im*, Ming-Chia Lai
Mechanical Engineering Depart., Wayne State University,
5050 Anthony Wayne Drive Detroit, Michigan 48202, USA
Suck-Ju Yoon
Mechanical Engineering Depart., Chonbuk National University, Chonju 561-765, Korea

The current trend in automotive finishing industry is to use more electrostatic rotating bell (ESRB) need space to their higher transfer efficiency. The flow physics related with the transfer efficiency is strongly influenced by operating parameters. In order to improve their high transfer efficiency without compromising the coating quality, a better understanding is necessary to the ESRB application of metallic basecoat painting for the automobile exterior. This paper presents the results from experimental investigation of the ESRB spray to apply water-borne painting. The visualization, the droplet size , and velocity measurements of the spray flow were conducted under the operating conditions such as liquid flow rate, shaping airflow rate, bell rotational speed, and electrostatic voltage setting. The optical techniques used in here were a microscopic and light sheet visualization by a copper vapor laser, and a phase Doppler particle analyzer (PDPA) system. Water was used as paint surrogate for simplicity. The results show that the bell rotating speed is the most important influencing parameter for atomization processes. Liquid flow rate and shaping airflow rate significantly influence the spray structure. Based on the microscopic visualization, the atomization process occurs in ligament breakup mode, which is one of three atomization modes in rotating atomizer. In the spray transport zone, droplets tend to distribute according to size with the larger drops on the outer periphery of spray. In addition, the results of present study provide detailed information on the paint spray structure and transfer processes.

Key Words : Electrostatic Rotating Bell, Paint Spray, Shaping Air

1. Introduction

The current challenges facing automotive finishing industry are ; (i) how to improve the finish quality, (ii) how to increase the paint transfer efficiency, and (iii) how to reduce volatile emissions without sacrificing the surface quality and the production line speed.

Although there has been a continuous demand of the surface quality in terms of color brightness and texture, it is well known fact (Bell and Hochberg, 1981) that the application of the ESRB systems results in a lower surface quality, especi ally for metallic painting, and produce a darker and duller appearance compared with the pneumatic spray gun. Two mechanisms are considered as possible reasons : First, the discoloration is due to improper flake orientation during fluid transportation, which is former thought in this field. Second, difference in the flake content in the deposited paint is the cause of the color shift (Inkpen and Melcher, 1987 ; Elmoursi and Lee, 1989 ; Tachi and Okuda, 1992). Based on the above discoloration mechanisms, improvement of the surface quality requires a better understanding

* Corresponding Author,
E-mail : ksim@eng.wayne.edu.
TEL : +1-313-577-5778; **FAX** : +1-313-577-5778
Mechanical Engineering Depart., Wayne State University, 5050 Anthony Wayne Drive Detroit, Michigan 48202, USA (Manuscript **Received** December 9, 2002; **Revised** September 17, 2003)

of the fluid transport process according to operational conditions and reformulation of the painting materials.

The paint transfer efficiency, defined as the ratio of the mass of solid paint deposited on the target to that dispersed from the applicator, is a metric for the efficiency of paint application process. One percent improvement in transfer efficiency of paint spray to target can potentially save millions of dollar per year in the cost of paint-shop bulk material. The reduced over-spray, thus increasing the transfer efficiency, allows a reduction in the booth downdraft and other compressed air flow usage, creating significant energy cost saving. In addition to the cost saving, higher transfer efficiency also has a corresponding reduction in the amount of volatile organic compounds (VOC) emissions, paint sludge production, and the associated after-treatment costs. While the optimal transfer efficiency claimed for ESRB applicators is higher than 90%, in a typical plant environment the actual efficiency is only about 75-80%. Thus, there has been a constant pressure to improve the transfer efficiency, which is significantly influenced by the operating parameters of an ESRB related to the application settings such as the airflow management (Tong et al., 1995), line-speed, and the shape of the surface being painted.

Therefore, the solution to the current challenges requires a research on the understanding of transfer processes, optimization of operating parameters, and new paint formulation (including the environmentally friendly paints, such as water based or powder paints) for the automotive painting, which is one of the most expensive facilities to maintain in an automotive manufacturing industry.

1.1 Historical perspectives

The use of a rotating cup in burners for domestic heating was well known in Europe in 1930s. Hinze and Milborn (1950) were among the first who documented the atomization process of rotating cup. Later on, Marshall (1954), Matsumoto et al.(1985), and Lefebvre (1989) summarized the earlier research activities about fluid atomization. In general, three different disintegration mechanisms were identified in atomization process, including a) direct drop formation at low feed rate, b) ligament breakup, and c) film breakup. In a generic atomizer, these three atomization mechanisms coexist. It was found that the transition from regime a) into b), or from b) into c) could be enhanced by adjusting the operational conditions ; 1) increase liquid feed rate, 2) increase the angular speed of the sprayer, 3) decrease the diameter of the sprayer cup, 4) increase the liquid density, 5) increase the liquid viscosity, and 6) decrease surface tension of the liquid employed.

Hinze and Milborn (1950) also measured the drop size in the ligament breakup mode by using a soot glass impingement technique. The data were correlated with relevant dimensionless groups, which set the standard for presenting the atomization data. Dombrowski and Lloyd (1974) visualized the atomization process using photography. They measured the drop size using a light absorption technique. In these earlier studies, however, smooth rotating cups without serration were usually used. The rotation speeds were also much slower than the turbine-driven applicators commonly used nowadays. In addition, electrostatics and shaping air control were rarely applied.

In addition to automotive painting, electrostatic atomization was widely used in agriculture spraying, office furniture refinishing, and ink jet printing. There was a long history of human interest in electrostatic atomizer. There were experiments about electrostatic atomization and the measurements of the associated particle charging before Benjamin Franklin's interest in electricity. Recently, Kelly (1994), and Okuda and Kelly (1996) have summarized the theories and practices of these early devices. Kelly found applications of electrostatic atomization as far back as two hundred and fifty years ago in Italy. From a theoretical viewpoint, he suggested that when the mean drop diameter of a Newtonian liquid was larger than one micron, the drop diameter was a function of fluid charging level only. All the other fluid and device related properties did not affect the mean drop diameter of the particles.

1.2 Previous studies in ESRB spray

Compared to the pneumatic spray gun, which is easier to set up and operate (e.g. Kowk and Liu, 1991 ; Dornnick et al., 1994), fewer research articles about the ESRB process are available.

Ransburg Corp., in 1960s, demonstrated that serrations machined into the inner edge of bell cup maintained the ligament break up regime well into the range of operating conditions, which normally produced sheet break up from a smooth bell cup edge. Hines (1966) studied the application of the electrostatic atomization to paint spray at Scientific Laboratory of Ford Motor Co. Atomization of single jets as well as atomization from rotating cups were investigated. The measurements of the mean drop size and the mean specific change were reported. His experiments resulted in a qualitative understanding of the influence of various operating parameters on the properties of paint spray. Dombrowski and Lloyd (1974) also visualized the atomization process using photography and measured the drop size using a light absorption technique.

Bell and Hochberg (1981) undertook the first major effort to investigate an ESRB application of metallic paint, simulating automotive production conditions. Their objective was to investigate the difference in color of coatings of the same paint applied by a pneumatic gun and an electrostatic rotating bell. Various experimental techniques including light scattering, Doppler methods, high-speed video, and charge/mass ratio measurements were employed. Based on the results, they postulated that the darker color produced by an ESRB was due to the large number of small drops (which did not contain any flake). These small drops were deposited by charging the drops in the ESRB spray but could be lost in overspray when applied by a pneumatic gun (Inkpen, 1986).

Inkpen and Melcher (1987) investigated the color difference problem further in an experimental study comparing metallic paint application by pneumatic gun and ESRB. An electrostatic shutter was developed to sample charged paint droplets depositing on an electrically grounded target. They observed that the mass percent of flake and average flake size deposited by a pneumatic gun were approximately twice those deposited by an ESRB. This was identified as the dominant mechanism for the color difference between coatings applied pneumatically and electrostatically. Their results discredited the popular notion that the color difference was caused by abnormal orientation of the flakes due to electrostatic forces in the paint film. The measurements also showed a wide variation in average flake size along the radius of deposited paint pattern. This observation underscored the important role played by droplet transport on the quality of the deposited coating.

Elmoursi and Lee (1989) used the electric shutter technique developed by Inkpen to study the influence of high voltage, bell rotational speed and bell-to-target gap on the flake size distribution. Their results indicated that the optimum values existed for all the three parameters at which both the drop size and the flake content were most uniform along the target surface.

Corbeels et al.(1992) used a laser diffraction instrumentation and photography to study the influence of fluid properties and operational parameters on the atomization characteristics of a high-speed rotary bell with serration, but without electrostatics and shaping air control. They found that the high viscosity fluid filmed the bell evenly and produced long regular ligaments, whereas the low viscosity fluid filmed incompletely and produced very irregular ligaments that disintegrated near the bell edge. Their particle size data, which were limited at one location (35 mm from the bell edge), were found to be insensitive to large changes in flow rate and viscosity at a bell speed higher than 20,000 rpm.

Fukuta et al.(1993) from Toyota Motor Corp. reported the development on a new bell for metallic paint application. This bell design was later modified to spray waterborne paint as well (Toda et al., 1994). They proposed that the deposited flake integrity and the orientation rather than the amount of flake caused the color difference. Their experiments showed that the critical factors in producing required flake deposition characteristics were bell tip speed and speed of the

paint drops near the target. The prototype bell was observed to produce a coating color similar to that by a pneumatic gun, but only at a transfer efficiency of 65%. It should be noted that this value was somewhat low for ESRB application that is capable of 90% transfer efficiency.

Bauckhage et al. (1994) used a short spark photography and a diffraction spectrometry to study the ESRB atomization of water based metallic paint. The small dispersion of the drop size distribution suggested that the ESRB works in the ligament atomization mode, which was confirmed by the photograph near the nozzle. They also used a laser light sheet for visualization; the unpublished video results suggested two axial zones and a radial zone of recirculations, which were influenced by the shaping air. Later, they also used a phase Doppler particle analyzer to study the effect of electrostatics and found that the drop size with higher voltage was smaller but the visualized spray cone was wider (Bauckhage et al. 1995).

While the operating parameters of an ESRB were closely related to transfer efficiency and surface quality, most of the previous studies used old applicators that did not have a control unit of a wide range of operation parameters. They only concentrated on the atomization aspects having very limited drop size data at one location and the visualization to the vicinity at the edge of the bell cup. New modified bell designs were introduced every year more from empirical experience and trial-and-error than from a scientific understanding of the processes. Moreover, the problem of color versus transfer efficiency associated with the ESRB application still persists. Detailed characterization of constituent processes, including initial atomization at the bell edge, the interaction with electrostatics and shaping air, the boundary layer formation, and deposition at the target are needed 1) to develop an efficient applicator without compromising color, and 2) to predict bell performance under various operating conditions.

1.3 Rotary atomization and electrostatic spray

When the liquid is supplied into the inside of a rotating cup as shown in Fig. 1, it will be shortly attained to the same rotational speed as that of the cup because of the friction between the liquid and the wall of the cup. If the rotational speed is fast enough, due to the viscous flow toward the sharp edge, the liquid will be arrived at the rim, become a thin continuous film, and eventually disintegrate into drops. In general, this depends on the cup size, rotational speed, liquid flow rate, and the liquid properties. Three different atomization modes can be observed around and beyond the edge of the cup (Hinze, 1950) depend on the rotational speed and the liquid flow rate; 1) direct drop formation, 2) ligament formation, 3) film formation.

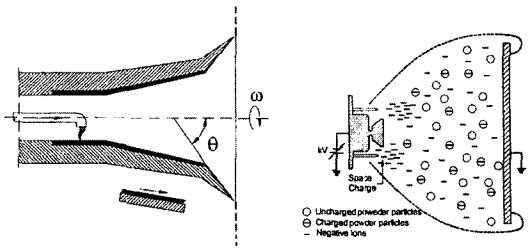

Fig. 1 The principle of the rotating cup atomization and the electrostatic spray

On the other hand, if the electrically conductive bodies with sharp tips bring into a high electric potential field, the high charge density will cause corona discharge. In this process, the ions will be formed continuously in the ambient atmosphere, which is called the air ionization. If then the liquid particles are brought into the charged air molecules, they will also be charged and transported to the grounded work-piece, which is charged the opposite potential. Note that the attraction depends on the existing potential difference.

2. Experimental Setup

2.1 The spray paint unit

A research paint booth completed with a digital controller for the ESRB is used for investigation. The bell assembly and a detail of the bell cup are illustrated in Fig. 2. In which, the high-

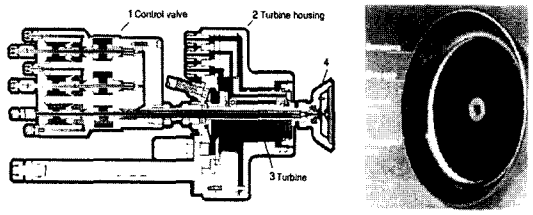

a) Main body b) Bell disk

Fig. 2 The main components of high speed rotating atomizer

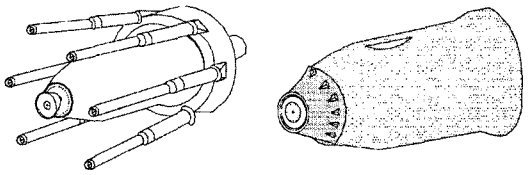

a) Waterborne bell atomizer b) Solventborne bell atomizer

Fig. 3 Two different electrostatic atomizers operated in typical paint spray

speed rotating atomizer consists of four components; 1) central control valve, 2) turbine housing, 3) turbine, and 4) bell disk.

The function of the central control valve is to control the material supply and return to/from the atomizer. The turbine housing protects the drive unit of the high-speed rotary atomizer. The compressed air driven by turbine powers the bell disk, which can be run up to a maximum rotating speed, through a hollow shaft.

The bell disk consists of four parts as shown in Fig. 2(b); central hole, ring gap, distributor ring, and serration. The paint flow is supplied to the atomizer ring by a ring gap and moves toward the bell edge due to the centrifugal forces created by the rotating bell. Many of the available bell disk variants have similar means for paint flow division, in which 80% of the paint quantity is supplied to the atomizer rim by the ring gap and the remaining 20% of the volume flow passes through the central hole on the front side of the distributor ring to affect a permanent rinsing of the bell disk surface to prevent paint deposits on the distributor ring. Small wedges, which are called serration or circumferential knurls (see also in Fig. 4), are designed along the edge of the bell disk. They permit the paint film flowing over the surface of the bell disk to be divided into defined individual flows and ligaments that eventually break up into droplets. Thus, the droplets obtained from the ligaments does not include any air pockets and become very uniform in size.

A production ESRB (Behr Eco-bell 55 mm diameter, serrated edge, designated 55S) for waterborne paint is chosen for the study. The major difference between solvent-borne base painting and waterborne base painting is in the electrical charging system and supplying component of the paint as shown in Fig. 3. In a solvent-borne base paint (Fig. 3(b)), due to the low conductivity of the solvent, the charging electrodes can be built into the applicator and provide a reliable electric field by conduction, induction, and corona current. However, waterborne paint requires external charging component, which is isolated from the paint supply system because of high conductivity of water.

Behind the rotating cup, shaping air is supplied from 40 holes, annularly arranged on the stationary housing. Shaping air is used primarily to support the transport of paint droplets, to stabilize the flow conditions around the atomizer, and to permit a precise alignment of the spray pattern by limiting the atomizing cone. The high voltage from the six external electrodes, which are negatively polarized and located at 75mm from the cup, charges the atomized droplets and propels them to the grounded work piece.

2.2 Microscopic visualization

Microscopic visualization was carried out to study liquid break up near the bell edge. A schematic of the visualization facility is shown in Fig. 4. The sampling area, 32 mm on the bell cup edge, was illuminated by 15 W copper-vapor laser (OXFORD, Model Cu-15A). The serrations continuously shaped by the peak and valley were clearly seen on the left side of Fig. 4. The beam from the pulse laser was transformed into a laser sheet using cylindrical lens and was focused on the sampling area. The CCD Camera (Kodak Megaplus ES 1.0) with a special long distance microscopic lens was used to obtain magnified im-

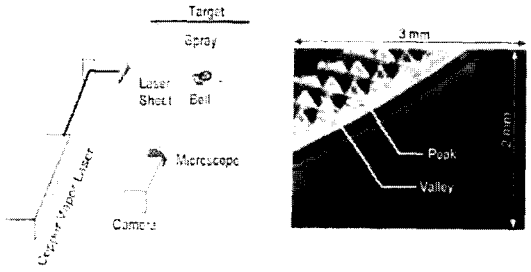

Fig. 4 The schematic of liquid breakup visualization on the bellcup edge

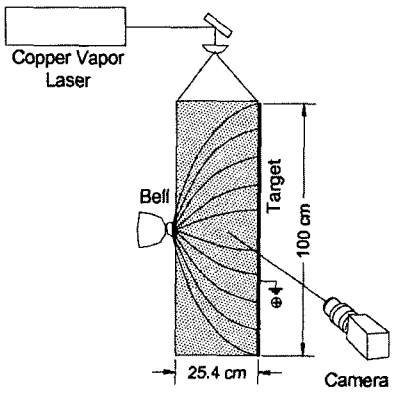

Fig. 5 The visualization set up of the spray

ages (at~100) at the bell edge. The laser was operated in single pulse mode to acquire a snap shot of rotating bell-cup edge and atomization. The images were recorded on a PC by an Image board (DT3752 Frame Grabber) through A/D converter. Later on, the image analysis was carried out for the saved digital images.

2.3 Spray visualization

The spray visualization was also carried out using a light sheet generated by the same copper-vapor laser operated at 10 kHz. The optics for generating light sheet was connected to the laser through a fiber-optic cable. The laser sheet was expanded to illuminate the center vertical plane, which covered the entire spray. The camera was positioned normal to the plane of light sheet to acquire images of spray structure. Either a digital Kodak Megaplus camera or a Nikon 35-mm SLR camera loaded with ISO-400 color film was used for taking the photograph. Figure 5 is a schematic of visualization of the spray photography.

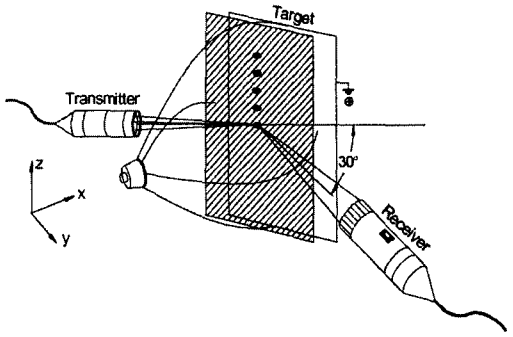

Fig. 6 The drop size measurement set up by the phase Doppler particle analyzer

2.4 Drop size measurement

Two-channel PDPA system (Aerometrics) was used for detailed measurements of the drop size distribution. Figure 6 is a schematic illustration of laser transmitter and receiver in a typical PDPA configuration. Two intersecting laser beams emanate from the transmitter and intersect at the focal point of the transmitting lens. A 300-mW Argon-ion Laser at 488 nm and 514.5 nm wavelengths was used as a light source. The focusing lenses of both the transmitter and receiver had a long focal length of 750 mm to avoid interfering with the spray. The optics was integrated with fiber optics cables and was mounted on a heavy-duty computer controlled traversing stand. Measurement data were taken along the axial direction and the different z-axis locations. Statistics at each point were averaged over 20,000 data points. The validation rate was higher than 90 percents for every measuring point. The different z-axis positions were presented for comparison in the parametric study.

2.5 Test conditions

Four main operating parameters were changed for the parametric study ; liquid flow rate, shaping air flow-rate, bell rotational speed, and high voltage setting. De-ionized water was used as a paint surrogate for simplicity. The target plane was located at 254 mm away from the edge of the rotary cup. A flat metallic panel (1.2 m 0.9 m, electrically grounded) was used as a target surface and the downdraft air was turned off. The temperature was set up at 213℃. The pressure was

Table 1 Test donditions

Liquid Flow rate(ml/min)	50	100	150	**200**	250
Shaping air flow rate(l/min)	120	140	150	**160**	180
Bell rotation speed(rpm)	20,000	30,000	**40,000**	50,000	
Voltage setting(kV)	0	60	70	80	**90**
Downdraft air flow rate(m/s)	0				
Booth condition	Normal ambient −21±3℃				
Liquid properties(water)	Surface tension=76m N/m				
	Viscosity=1.0 mNs/m^2				

kept on ambient condition in the spray booth. The test conditions are summarized in Table 1.

The following reference conditions were selected as a baseline in this parametric study ; liquid flow rate at 200 ml/min, shaping air flow rate at 160 l/min, bell speed at 40,000 rpm, and high voltage setting at 90 kV. These baseline set of conditions are also underlined and bold-faced in Table 1. In order to discern the effect of changing main operating parameters, only one parameter was changed at a time, while the other three were maintained at the baseline condition.

3. Results and Discussion

3.1 The characteristics of the paint spray

Figure 7 shows the PDPA results at the reference condition superimposed on the spray light sheet photograph. The measurement data were taken along the axial direction at x=2.5, 10.2, 17.8, and 24.1 cm from the bell cup edge and at the radial locations of r=0, 10.2, 20.3, 30.5 and 40.6 cm. The measured Sauter mean diameter (SMD) is proportional to the size of circle plotted at each measuring position ; the measured two directional velocities are also plotted as a vector. An important observation from Fig. 7 is that a re-circulating flow, which is dominating on the plane of the bell cup centerline axis, is created between the bell cup and the target due to strong shaping air flowing over the bell cup. In addition, the strong rotating swirling flow induced by high bell speed is located on the perpendicular plane of bell centerline axis. The vector plot in Fig. 7 combined with the visualization results gives rise to the conceptual streamline plot, which is similar to the

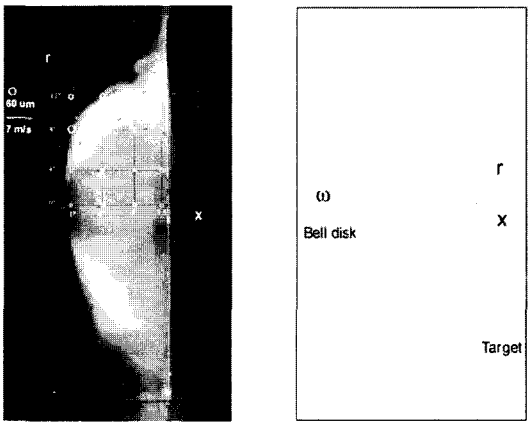

Fig. 7 Typical ESRB spray flow with conceptual streamline plot

one proposed by Bauckhage et al. (1994). Figure 7 also shows that the larger droplets stay on the outside of the spray, while smaller droplets are more easily entrained into the re-circulating zone. As the penetration length increases, the radial diameter profile becomes more uniform (also see in Fig. 8).

Figure 8 shows a variation of droplet concentration, velocity and mean diameter in the center vertical section of the spray at 30,000 rpm bell speed, 150 l/min shaping air flow rate, 50 ml/min liquid flow rate and a charging voltage of 90 kV ; Fig. 8(a) is an image of the spray taken with laser light sheet visualization, where the dark areas represent the droplet concentration ; Fig. 8(b) depicts droplet mean velocity vector plot with vertical and axial components ; a plot of droplet SMD is shown in Fig. 8(c).

In the re-circulation zone, the concentration of drops is low as seen in the image (Fig. 8(a)). The bulk of the drops are distributed along the edge of spray, which widens from the bell to the target. The maximum value of drop size and velocity is observed near the bell edge, and decrease towards the target as the spray becomes wider. At the edge of the rotary bell, breakup point, the droplet velocity is almost perpendicular to the bell axis, as shown by the large vertical component in Fig. 8(b). As the drops move away from the bell, immediately, two forces, the shaping airflow and the electrostatic force are infl-

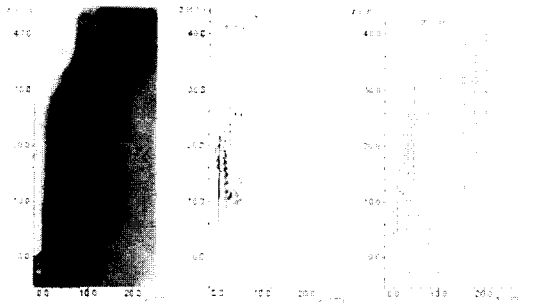

(a) Spray conentration (b) Drop mean velocity (c) Drop mean diameter

Fig. 8 The spray structure at the condition of 50 ml/min liquid flow rate 150 l/min, shaping air, 30 k rpm bell speed, and 90 kV voltage setting

uencing to them, and thus the axial velocity toward the target will be increased. However, the magnitude of total velocity is rapidly reduced due to aerodynamic drag within short distance from the bell edge.

The trajectory of each droplet is dictated by the relative magnitude of the forces acting on it, that is, inertia, aerodynamic and electrostatic. The balance among these forces moves depending on drop size, causing the drops to segregate within the spray. The measurement of the drop size (Fig. 8(c)) shows that the re-circulation zone contains mostly the smallest drops while larger drops are accumulated on the outside of the spray flow.

3.2 Microscopic visualization

Figure 9 shows the microscopic visualization images on different bell speed keeping the liquid flow rate 50 ml/min. At 20,000 rpm in Fig. 9(a), the ligaments are starting to create from the serrations on the bell edge. Moreover, they are uniformly spaced, coinciding with spacing of serrations, which are indicating uniform sizes in diameter but the bell speed does not seem to be sufficient for fine spray. At 30,000 rpm, the uniform spacing is still preserved, but the ligaments are relatively longer and thinner in Fig. 9(b). At 40,000 rpm, the formation of multiple ligaments is observed between serrations, and consequently, the ligament diameter decreased further. This trend indicates that the drop size decreases with

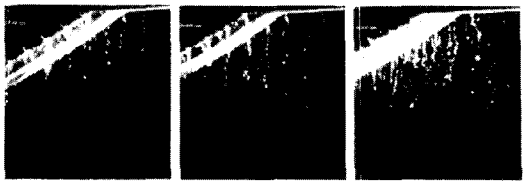

(a) 20,000 rpm (b) 30,000 rpm (c) 40,000 rpm

Fig. 9 Microscopic visualization on the bell speed at the liquid flow rate=50 ml/min (Magnification=100x)

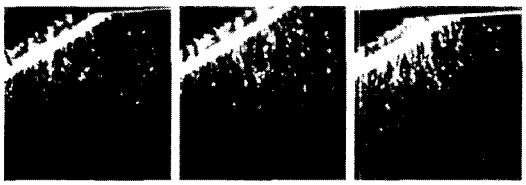

(a) 150 ml/min (b) 250 ml/min (c) 350 ml/min

Fig. 10 Microscopic visualization on the liquid flow rate at the bell speed=20 k rpm (Magnification=100 x)

increase in bell rotating speed.

When the liquid flow rate is increased keeping bell speed constant as seen Fig. 10, the filaments are formed in increasing numbers with irregular spacing and non-uniform of ligament diameters. Note that the ligaments are also seen to interact with each other before breakup. In addition, it is clearly observed that the non-uniformity of ligament formation is increased with flow rate.

3.3 Spray visualization

Figure 11 to 14 show the effects of operation parameters on the overall axial spray pattern, which are photographed with the SLR camera with an exposure time of 33.3 ms. The short exposure time does not allow enough time averaging; however, sufficient information can be obtained from the image. The spray cone angle, i.e., θ, taken to be the angle between the spray trajectories from the edge of the bell cup to that of the ESRB centerline, is also measured directly from the photograph and plotted in Fig. 15. The error percent of the spray angle, which is measured 10 times for each image from five different snapshots, is ranged from 1.1% to 2.5% for the standard mean values.

The results show that an increase in liquid low-rate from 100 ml/min to 250 ml/min [Figs. 11(a) to (d)] while keeping the other three parameters at reference condition tends to widen the spray shape slightly. This is due to a higher spray swirl momentum associated with the increased spray mass and possibly large droplet size. It is also noted that the most spray mass concentrates on the outside of the spray when increasing the flow rate.

Figures 12(a) ~ (d) demonstrate the effects of shaping air. At higher flow rate of shaping air, the spray cone is generally narrower. This is particularly obvious when comparing Figs. 12(a) (120 l/min) and 12(b) (140 l/min). In case of 120 l/min, a lot of spray masses pass over the target, which increases the overspray. This important observation indicates that the shaping air should operate higher than 120 l/min in terms of spray transport. From this analysis, the shaping air permits precisely adjustment of the spray pattern by limiting the spray cone angle ; it also increases impinging energy at the target (see in Fig. 12(d)).

The influence of bell speed on the overall spray pattern is shown in Figs. 13(a) ~ (d). At the low bell speed of 20,000 rpm, where the centrifugal force is the smallest, large droplets are clearly observed outside of the denser and finer spray region, unaffected by the shaping air.

These large droplets suggest that the atomization mode is not well developed. At the bell speed of 30,000 rpm, the spray becomes tender and makes cone shape. From this analysis, it seems to have critical change between 20,000 rpm and 30,000 rpm. Therefore, it is recommended that the ESRB must be operated at a speed higher than 20,000 rpm. At higher bell speed when centrifugal force is larger, the spray cone decreases due to more consistent and finer atomization. The spray also tends to concentrate more inside the spray cone as a greater number of smaller particles find themselves into the re-circulating zones.

(a) 100 ml/min (b) 150 ml/min (c) 200 ml/min (d) 250 ml/min

Fig. 11 The effects of the liquid flow rate : shaping air=160 l/min, bell speed=40 k rpm, and voltage setting=90 kV

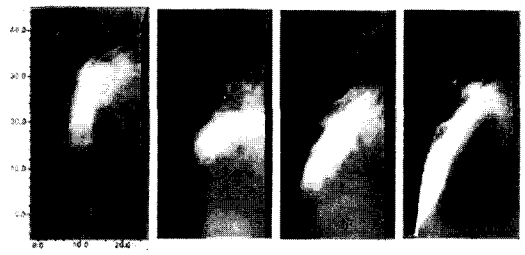

(a) 120 l/min (b) 140 l/min (c) 160 l/min (d) 180 l/min

Fig. 12 The effects of the shaping air flow rate : liquid flow rate=200 ml/min, bell speed= 40 k rpm, and voltage setting=90 kV

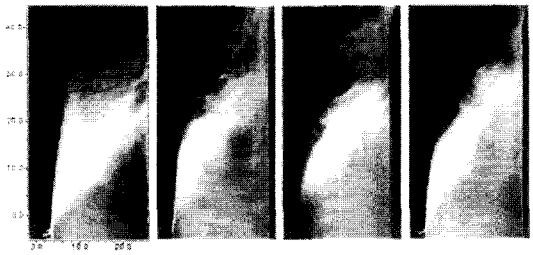

(a) 20,000 rpm (b) 30,000 rpm (c) 40,000 rpm (d) 50,000 rpm

Fig. 13 The effects of the bell speed : liquid flow rate=200 ml/min, shaping air=160 l/min, and voltage setting=90 kV

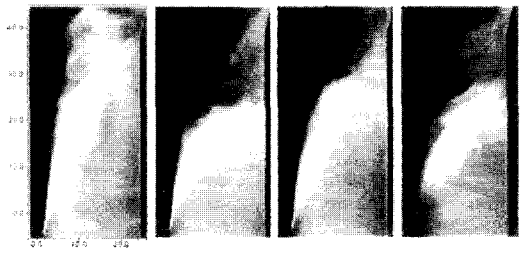

(a) 60 kV (b) 70 kV (c) 80 kV (d) 90 kV

Fig. 14 The effects of the high voltage : liquid flow rate=200 ml/min, shaping air=160 l/min, and bell speed=40 k rpm

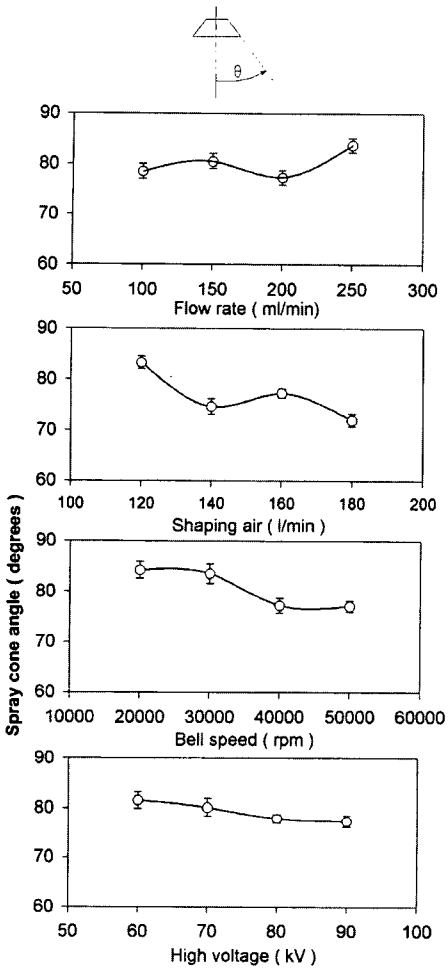

Fig. 15 Sensitivity of the bell operation parameter on the spray cone angle

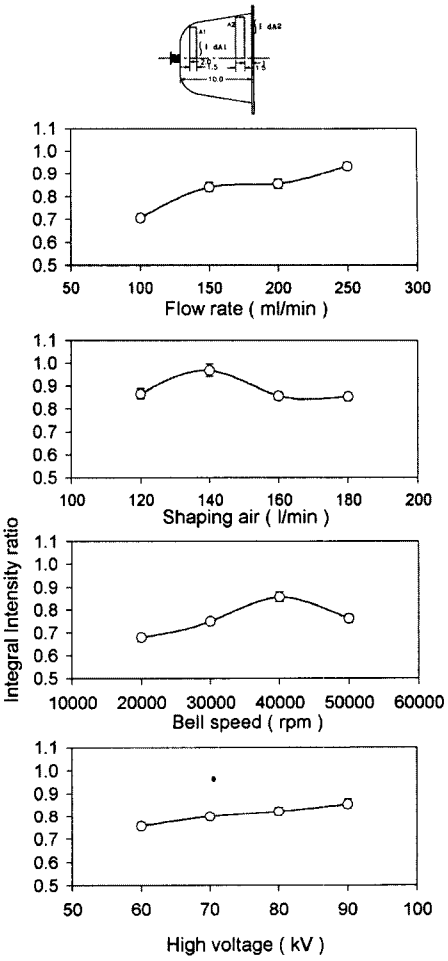

Fig. 16 Sensitivity of the bell operation parameter on integral intensity

The influence of the high voltages on spray shape is shown in Figs. 14(a) ~ (d). Insufficient high voltage exerts only small forces on the droplets, resulting in wider spray and poorer transfer efficiency. At the highest voltage, the spray also becomes denser and more uniform at the core region.

Since the actual transfer efficiency is difficult to measure, a simple image analysis can be used to aid its estimation. Intensity integration is taken over two rectangular areas within spray. Both are 5.1-cm wide, one taken at 2.5 cm from the target plane, the other at 3.8 cm from the bell cup. The ratio of two should give some relative indication of transfer efficiency, assuming the laser light sheet is uniform in these areas and the spray is relatively steady. The results are plotted in Fig. 16. The results show that the liquid flow rate and the high voltage setting affect the spray transport with increasing the integral intensity values according to increase the operating parameter. Also, the integral intensity ratio shows an opposite trend with respect to spray cone angle, in their response to bell speed and high voltage setting.

3.4 Drop size measurement

Figures 17 and 18 plot the PDPA measurements of the parametric study, taken at 7.6 cm from the target plane, in terms of radial profiles of volume-averaged drop size and mean. An increasing the

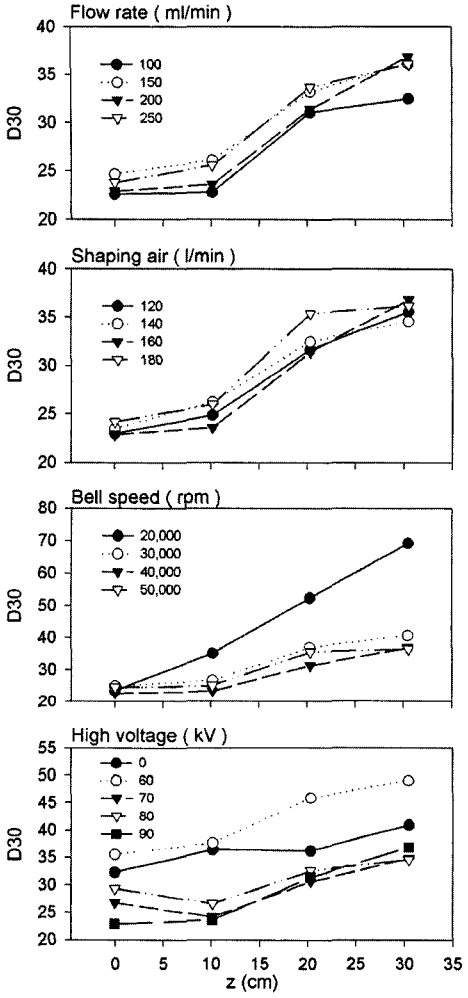

Fig. 17 The effects of the bell operation parameters on the drop size profile measured at 7.62 cm from the target

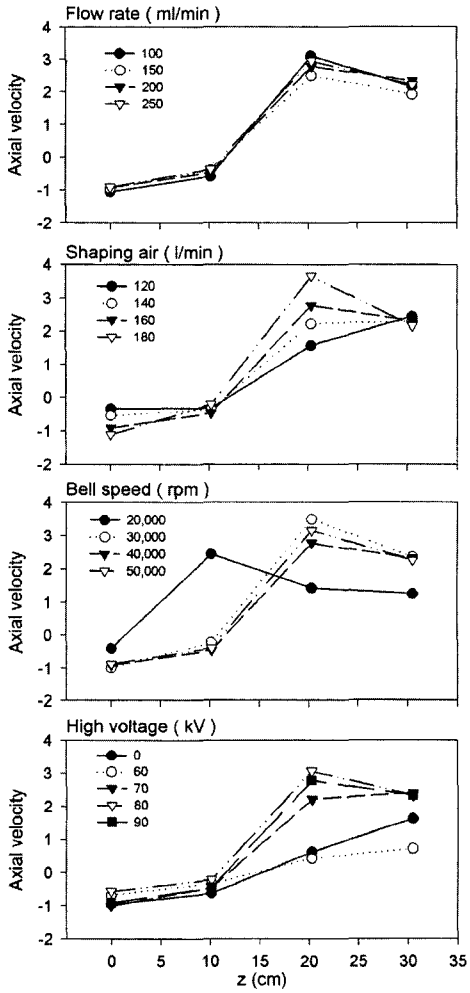

Fig. 18 The effects of the bell operation parameters on the axial velocity at 7.62 cm from the target

flow rate from 100 ml/min to 250 ml/min while keeping the other parameters under the reference conditions does not have an obvious effect on drop size or velocity except at the outer edge of the spray. However, the shaping air has more significant effects on velocity than drop size, confirming that its primary function is more in directing spray transport than in assisting atomization.

As far as the atomization processes are concerned, the bell speed is the most important influencing parameter. For example, if the bell speed is increased, the droplet size should be decreased. Although too fine spray may lead to overspray and non-uniform coating thickness because the small droplets are easily influenced by air flow in the booth. On the other hand, if bell speed is too lower, it may result in coarse distribution because of the insufficient atomization process. At the bell speed of 20,000 rpm, particle sizes are varied from 25 μm at the center to 73 μm at the edge of the spray, indicating that the atomization process is not well developed at this condition which is unsuitable for practical painting purposes. Although, the other conditions seem to be suitable.

Similar to the flow visualization result, there

is a pronounced effect on the drop size and velocity when the bell speed increases from 20,000 to 30,000 rpm, strongly indicating a critical speed in between at which transition of the atomization mode occurs. The effect of high voltage is also very significant, but becomes marginal when the voltage is higher than 70 kV. The fact that the mean drop size at 60 kV is larger than those at 0 kV is not an indication that electrostatic atomization does not occur, but a result of the larger droplets being driven to the target plane. The PDPA data, again, is consistent with the choice of optimal condition, which is a trade-off to satisfy both atomization and transport requirements.

3.5 The spray distribution

The histogram data of the reference condition are shown in Fig. 19, corresponding to the measurements shown in Fig. 7. There is a notably bimodal distribution at the maximum drop size/velocity point. This distribution is also observed at the low-speed regime in Fig. 20(a) and at low voltage condition in Fig. 20(b), all taken at 7.6 cm from the target plane. The reason for this interesting bimodal distribution is unclear. It may be due to a dual-mode operation of ESRB atomization or transtion from the ligament atomization to the film atomization, where both the ligament and the film breakup mode coexist. Although it could also be due to a secondary breakup process where much distinctly smaller satellite drops are formed. The swirling and re-circulation flow field will also differentiate and transport the droplets according to their size and drag. Therefore, more study is required to solve this puzzle. Except these bimodal distributions, the other histograms of the drop size distributions have similar trends. It can be modeled to probability distribution function (PDF) for the numerical simulation, where the particle injection will be assumed to a-squared distribution or log normal distribution function.

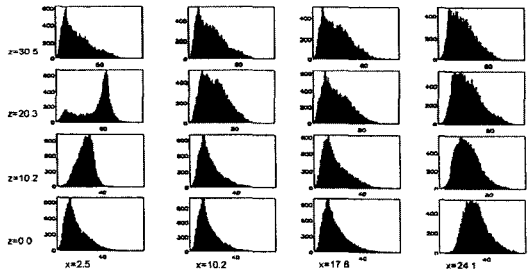

Fig. 19 The spatial distribution of drop size histogram at reference conditions

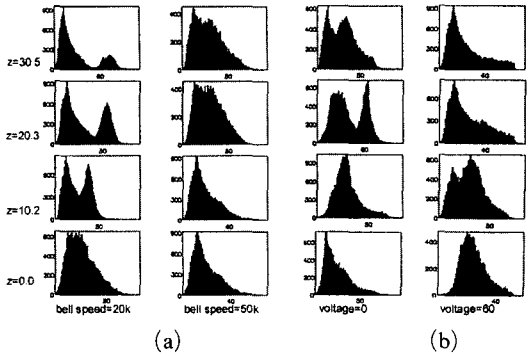

(a) (b)

Fig. 20 The drop size histogram variation at 7.62 cm from the target plane: (a) bell rotating speed, (b) high voltage setting

4. Conclusions

A parametric study was carried out to understand the paint spray structure and transfer process of the automotive electrostatic rotary bell applicator. The experimental techniques used in this study are the microscopic visualization, laser light sheet visualization, and a phase Doppler particle analyzer. The following conclusions can be made from the experimental study.

The present results showed that the most influencing parameter on the atomization process is the bell speed. Especially, based on the visualization and size measurement results, an operating condition should avoid a practically unsuitable condition, which is showed the very coarse size distribution.

The liquid flow rate is related with atomization in the sense that the non-uniformity of ligament formation increased with flow rate. Also, it modifies the spray pattern based on the visualization image analysis.

The high voltage and the shaping airflow rate significantly modify the spray transport. However, at lower voltages, i.e., changing from 60 kV to 70 kV, the electric force seems to affect the

atomization process.

The results of this study also provide detailed information on the paint spray structure and transfer processes, which can be used in numerical model development and validation.

Reference

Bauckhage, K., Scholz, T. and Schulte, G., 1994, "Atomization of Water-based Metallic Paints by Means of Electrostatic Rotary Atomizers," *Proceedings of ICLASS-94*, pp. 1010~1019, July 18-22, 1994, Rouen, France.

Bauckhage, K., Scholz, T. and Schulte, G., 1995, "The Influence of Applied High-Voltage on the Atomization Characteristic of a Commercial High-Speed Rotary Atomizer," *4th International Congress Optical Particle Sizing*, Nurnberg, Germany, 21-23 March 1995, pp. 337~346.

Bell, G. C. and Hochburg, J., 1981, "Mechanisims of Electrostatic Atomization, Transport, and Deposition of Coating," *Proceddings of Seventh International Conference in Organic Science and Technology*, Athens, Greece.

Corbeels, P. L., Senser, D. W. and Lefebvre, A. H., 1992, "Atomization Characteristics of a High Speed Rotary Bell Paint Applicator," *Atomization and Sprays*, Vol. 2, pp. 87~99.

Dombrowski, N. and Lloyd, T. L., 1974, "Atomization of Liquids by Spinning Cups," *Chemical Engineering Journal*, Vol. 8, pp. 63~81.

Domnick, J., Lindenthal, A., Mundo, C., Ruger, M. and Sommerfeld, M., 1994, "Combined Experimental and Numerical Investigations of the Spray Coating Process," *7th Int. Coating Process Science and Techn. Symp.* Atlanta, April 18~21.

Elmoursi, A. A. and Lee, H. Y., 1989, "Droplet and Flake Size Distribution in the Electrostatic Spraying of Metallic Paint," *SAE paper* 890354.

Fukuta, K., Murate, M., Ohhashi, Y. and Toda, K., 1993, "New Electrostic Rotary Bell for Metallic Paint," *Metal Finishing*, October, 1993, pp. 39~42.

Hines, R. L., 1996, "Electrostatic Atomization and Spray Painting," *J. Applied Phys.*, Vol. 37, pp. 2730~2736.

Hinze, J. O. and Milborn, H., 1950, "Atomization of Liquids by Means of a Rotating Cup," *Journal of Applied Mechanics*, Vol. 17, pp. 145~153.

Inkpen, S. and Melcher, J. R., 1987, "Dominant Mechanisms for Color Differences in the Mechanical and the Electrostatic Spraying of Metallic Paints," *Industrial Engineering Chemistry Research*, Vol. 26, pp. 1645~1653.

Kelly, A. J., 1994, "On the Statistical Quantum and Practical Mechanics of Electrostatic Atomization," *Journal of Aerosol Science*, Vol. 25(6), pp. 1159~1177.

Kwok, K. C. and Liu, B. Y. H., 1991, "New Research Approach to Air Spray Painting," *Proceedings of ICLASS-91*, Gaithersburg, MD, pp. 105~112.

Lefebvre, A. H., 1989, *Atomization and Sprays*, pp. 189~193, 222~228, Taylor and Francis, Bristol, PA.

Marshall, W. R., 1954, "Performance Characteristics of Spinning-Disk Atomizers," *in Chapter 3 of Atomization and Spray Drying*, Republished by Johansen Crosby & Assoc., Inc., Madison, WI, 1986.

Matsumoto, S., Belcher, D. W. and Crosby, E. J., 1985, "Rotary Atomizers : Performance UnderstandingandPrediction," *Proceedings of ICLASS-85*, Madison, WI, pp. 1A/1/1~21.

Okuda, H. and Kelly, A. J., 1996, "Electrostatic Atomization-Experiment, Theory and Industrial Applications," *Physics of Plasmas*, Vol. 3(5), pp. 2191~2196.

Tachi, K., 1985, "Effect on Rotating Cup Shapes and Spray Conditions on Spray Atomization," *J. of the Japan Soc. of Colour Material*, Vol. 58(7), 1985.

Tachi, K. and Okuda, C., 1992, "Color Variation of Automotive Metallic Finishes," *Journal of Coatings Technology*, Vol. 64(811), pp. 64~77.

Tong, E., Chmielewski, G. and Nivi, H., 1995, "Paint Spray Airflow Management," *Proceedings of International Body Engineering Conference & Exposition (IBEC 95)*, pp. 39~49, Oct. 31-Nov. 2, 1995, Detroit, MI, USA.